
Title: The concavity of modern submarine canyon longitudinal profiles

Authors: Euan L. Soutter[1], Ian A. Kane[1], David M. Hodgson[2], Stephen Flint[1],

Institutions: [1]Department of Earth and Environmental Sciences, University of Manchester, Manchester, M13 9PL, U.K.

[2]School of Earth and Environment, University of Leeds, Leeds, LS2 9JT, U.K.

Email: euan.soutter@manchester.ac.uk [Euan L. Soutter]

KEY POINTS

- 555 submarine canyon longitudinal profiles and their concavities have been measured
- Tectonics is the primary control on canyon concavity, with forearcs hosting the least concave canyons and passive margins the most concave
- Onshore climate noticeably affects the concavity of canyons formed adjacent to landmasses subject to major Quaternary ice loss

ABSTRACT

Submarine canyons incise into continental shelves and slopes, and are important conduits for the transport of sediment, nutrients, organic carbon and pollutants from continents to oceans. Submarine canyons bear morphological similarities to subaerial valleys, such as their longitudinal (long) profiles. Long profiles record the interaction between erosion and uplift, making their shape, or concavity, a record of the environmental and tectonic processes that canyons are subject to. The processes that govern concavity of subaerial valleys and rivers are well-documented on a global-scale, however, the processes that control submarine canyon concavity are less well constrained. We address this problem by utilizing existing geomorphological, tectonic and climatic datasets to measure the long profiles and quantify the concavities of 555 modern submarine canyons. Key results show that: 1) the dominant control on submarine canyon concavity is tectonics, with passive margins hosting the most concave-up profiles, and forearcs hosting the least concave-up profiles; 2) present-day canyon position affects canyon concavity, with river-associated canyons showing greater morphological variance than canyons currently dissociated from rivers; and 3) canyons subject to major Quaternary glacial runoff show increased concavity, suggesting onshore climate affects canyon concavity through sediment supply variation. These results show that tectonic and climatic processes are recorded in the morphologies of submarine canyons on a global-scale, and that many canyons have been slow to respond to sea-level rise since the Last Glacial Maximum.

PLAIN LANGUAGE SUMMARY

Submarine canyons are primarily formed by erosion beneath dense underwater mixtures of sediment and water transported into the sea by rivers, and submarine landslides. The record of erosion and deposition from these flows is preserved in the downstream, or longitudinal, profile of the submarine canyons they form. Submarine canyons are also affected by tectonic processes, such as seabed faults, which deforms their longitudinal profiles. Since these tectonic and sedimentary processes vary globally, we wondered whether this variation is reflected in the longitudinal profiles of submarine canyons globally. We found out that in places where tectonic activity is great, such as Western South America, submarine canyons tend to have more linear downstream profile, while in places where tectonic activity is low, such as Eastern North America, submarine canyons tend to have a more concave-up profile. We also found evidence that many canyons still have the same profile as they did during the Last Glacial Maximum, when sea-level was much lower, indicating that they have been slow to respond to climate change. Submarine canyons therefore tend to have different shapes depending on where you are on the Earth's surface, which results from the different sedimentary and tectonic processes they are subject to.

KEYWORDS

Submarine canyons, longitudinal profiles, concavity, tectonics, sea-level, Quaternary

TEXT

1. Introduction

The relationship between the elevation of subaerial valleys and channels, and downstream distance (e.g. Yatsu, 1955; Dietrich et al., 2003; Whipple and Tucker, 1999), and submarine canyons and channels, and downstream distance (e.g. Adams and Schlager, 2000; Pirmez et al., 2000; Huyghe et al., 2004; Mitchell, 2005; Gerber et al., 2009; Covault et al., 2011; Georgiopoulou and Cartwright, 2013) is expressed in their longitudinal, or 'long', profile. Long profiles record the interaction between uplift or base-level change, which are primarily controlled by tectonics and climate (e.g. Whipple and Tucker, 1999), and the erosive potential of flows passing through the channel, primarily controlled by sediment supply, sediment character and discharge (e.g. Snow and Slingerland, 1987). Therefore, long profiles have been used extensively to assess landscape evolution (e.g. Mackin, 1948; Ouchi, 1985; Sklar and Dietrich, 1998; Snyder et al., 2000; Roberts and White, 2010).

Subaerial long profiles tend to evolve through an inverse power-law relationship between the profile slope and drainage area, i.e., long profiles flatten downstream as the contributing drainage area increases. The rate at which a long profile flattens downstream is known as its concavity (e.g. Zaprowski et al., 2005), and is often used to describe the shape of a long profile (e.g. Sinha and Parker, 1996; Roe et al., 2002). Under steady-state conditions, when uplift equals erosion, long profiles tend to be concave-up, while under non-steady-state conditions, often driven by base-level change or tectonic deformation (e.g. Whipple and Tucker, 1999), profiles tend to be less concave, or convex-up. Spatial and temporal changes in long profile concavity can therefore be used to assess the influence of external processes acting on the profile. Rivers flowing across active faults in Italy, for example, are more convex than those flowing over relatively inactive faults (Whittaker, et al., 2008), and rivers in eastern North America become more concave with increasing precipitation (Zaprowski et al., 2005).

This concept has also been applied at a global-scale, with rivers formed in arid environments found to have decreased concavity (Chen et al., 2019) and rivers formed in tectonically-active environments found to have increased concavity (Seybold et al., 2020). This observation was demonstrated theoretically by Seybold et al. (2020), who derived the elevation of a long profile as a function of the uplift gradient (Δ):

$$S(x) = \left(\frac{\bar{U} k_H^{m/h}}{k}\right)^{1/n} \left(\frac{1-2\Delta\frac{x-\bar{x}}{L}}{x^{m/h}}\right)^{1/n} \quad \text{(Eq. 1)}$$

where S is the profile slope, x is downslope distance, $\bar{x}$ is the midpoint of the profile, L is the length of the profile, $\overline{U}$ is the mean uplift rate, k_h is a scaling coefficient, k is the erosional efficiency coefficient, h is the Hack exponent, Δ is a dimensionless parameter that controls how $\overline{U}$ varies along the river profile (the uplift gradient), and m and n are positive exponents. A long profile is obtained from Eq 1. by integrating from the most upstream point of the profile (x_0) to the most downstream point of the profile ($x_0 + L$) (Fig. 1A). Using this derivation, Seybold et al. (2020) showed that more convex profiles are expected to form when tectonic uplift is focused in the upstream parts of a channel, indicating that on a global-scale rivers in tectonically-active environments are predominantly affected by uplift in their upstream extents (Fig. 1A).

While subaerial valleys and submarine canyons are formed by different sedimentary processes, they both evolve in superficially similar fashions, with both being subject to substrate erosion by streamflow along their thalweg and retrogressive slope failure along their margins (Mitchell, 2004, 2005). In submarine environments an exponential decay in transport capacity downstream (Adams and Schlager, 2000) has been proposed as a control on the formation of longitudinal profiles similar in shape to subaerial profiles (e.g. Primez et al., 2000; Covault et al., 2011). Utilizing methods commonly applied to subaerial systems has led to insights into the processes and evolution of submarine canyons (e.g. Ramsey et al., 2006; Gerber et al., 2009; Covault et al. 2011; Amblas et al., 2012; Brothers et al., 2013). The different impinging processes, such as background sedimentation (e.g. Gerber et al. 2009), the paucity of direct measurements, and reduced bathymetric resolution, however, has made the controls on submarine long profile shape more difficult to constrain than their subaerial counterparts.

The global variability of submarine concavities has been studied previously by Covault et al., (2011), through the analysis of 20 present-day canyons, and by Adams and Schlager (2000), through the analysis of 150 seismic profiles of submarine slopes. This study aims to expand on this earlier work by measuring 555 long profiles and their concavities, extracted from an existing map of present-day submarine canyons (Fig. 2A; Harris and Whiteway; 2011). Climatic, oceanographic and tectonic datasets are also incorporated, with the aim of: 1) measuring the global distribution of submarine canyon concavities, and 2) assessing the dominant controls on modern submarine canyon concavity at a global- and continental margin-scale.

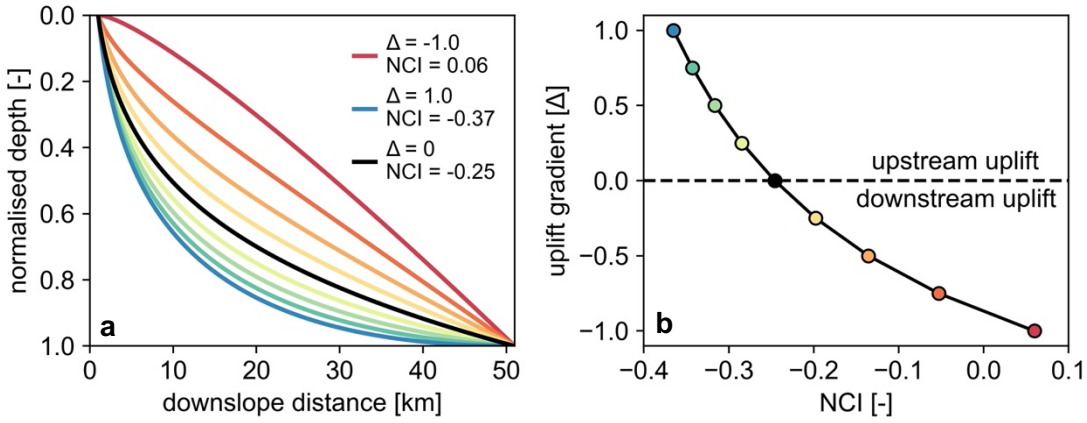

Figure 1: A) The long profiles of a 50 km long canyon subject to varying uplift gradients (Eq. 1). Upstream uplift results in concave profiles with low NCI values (B), and downstream uplift results in convex profiles with high NCI values (B). Depth instead of elevation is plotted to visualise a submarine profile. Parameters are: $\overline{U}$ = 1 mm yr^{-1}, x_0 = 1 km L = 50 km, k = 10 mm yr^{-1} km^{-1}, k_h =1 km $^{-0.2}$, m = 0.5, n = 1, h = 0.6.

2. Methodology

2.1 Submarine canyons

The global distribution of modern submarine canyons, and their positions, spacings, average sinuosities, dendricities (number of tributary canyons), and gradients were measured by Harris and Whiteway (2011) (Fig 1A). Canyons were mapped by Harris and Whiteway (2011) through automated drainage path analysis and manual mapping of the 1 arc-minute (0.017°) ETOPO1 global bathymetric relief map (Amanke and Eakins, 2009) (Fig. 2). The ETOPO1 map is a stitched compilation of different bathymetric data sources, such as the General Bathymetric Chart of the Oceans (GEBCO) and the US Coastal Relief Model (NGDC). The ETOPO1 map is formed by either gravity-constrained or sounding-constrained interpolation between direct measurements derived from ship-track soundings (Fig 1).

The mapping by Harris and Whiteway (2011) required certain criteria to be met, with each canyon: 1) spanning > 1000 m depth range, 2) having a width/depth ratio less than 150:1, 3) incising greater than 100 m into the seafloor throughout their length, and 4) having a head that is shallower than 4000 m below sea-level. Canyons formed on abyssal relief, such as midocean ridges and seamounts ('non-margin' canyons or channels; Peakall and Sumner 2015), were also excluded. These criteria are enforced by data resolution and therefore necessarily exclude some canyons. It is expected, however, that the consistent approach will yield representative trends. Canyon tributaries mapped by Harris and Whiteway (2011) are not used in this study, only the main canyon profile is analyzed. Tributary data along the length of the main canyon are instead accounted for by dendricity measurements.

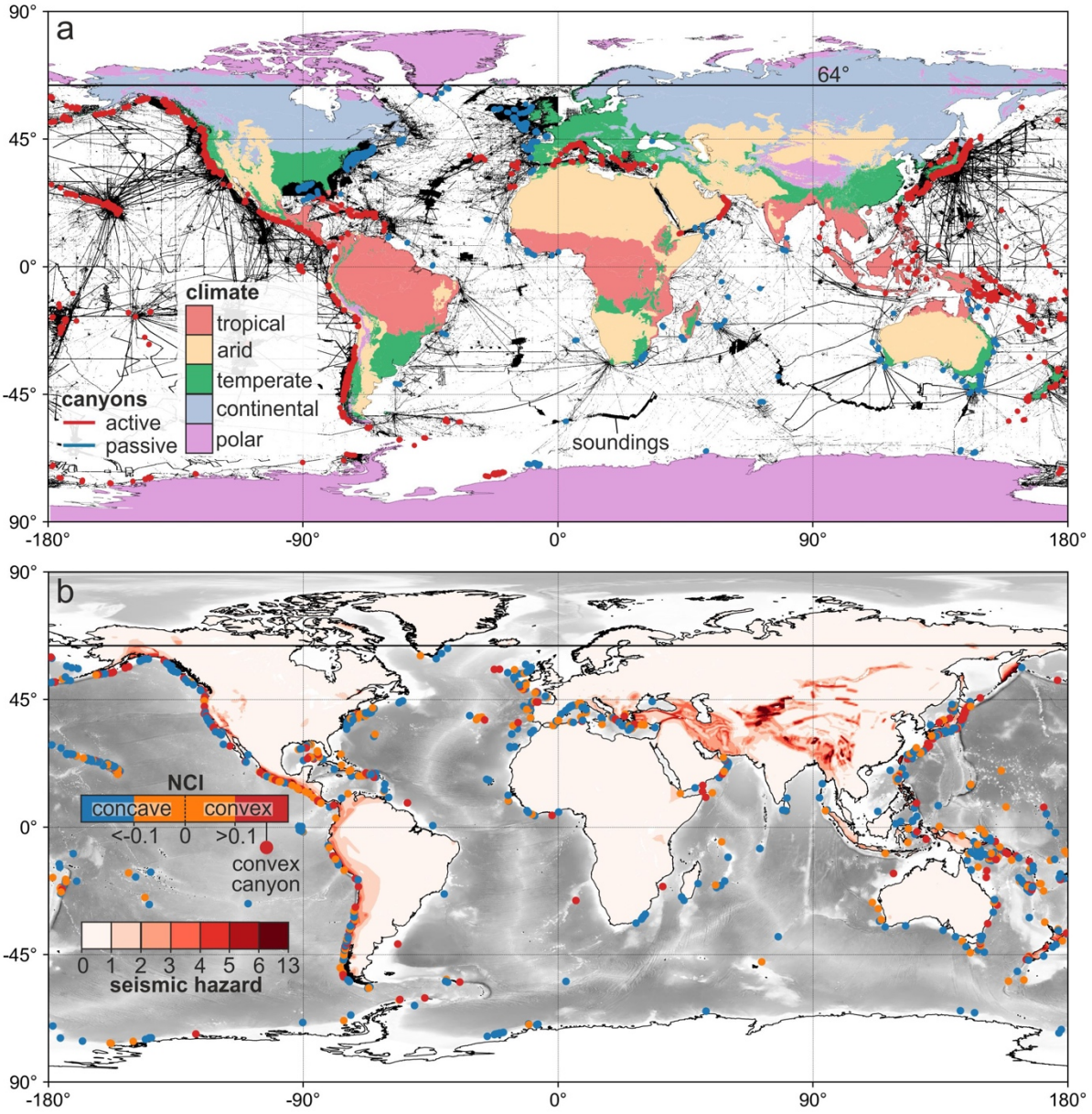

Figure 2: a) The submarine canyons (Harris and Whiteway, 2011), bathymetry (ETOPO1; Amanke and Eakins, 2009) and seismic hazard (Giardini et al., 1999) used in this study. Red lines indicate canyons formed on active margins and blue lines indicate canyons formed on passive margins or tectonically-quiescent basins (as defined by Nyberg et al. 2018). b) Submarine canyon concavities measured by this study (each canyon centred on a single point for clarity).

2.2 Longitudinal profiles and the normalised concavity index (NCI)

Long-profiles were extracted from each canyon by sampling the depth of the canyon trace over the ETOPO1 bathymetry (Amanke and Eakins, 2009), on which the canyons were originally mapped (Fig. 2A; 3; 4). Canyon traces were sampled at 0.01° (~1 km) intervals on a WGS-84 projection, with the metric distance between each point measured using Vincenty's geodetic formulae (Vincenty, 1975). This resulted in differences in measured lengths between Harris and Whiteway (2011), who used a different method, and this study (Fig. S2). In order to mitigate against the potential for profile smoothing by mapping across lower-resolution sections of the ETOPO1

map, only canyons constrained by a sounding at their mid-point were analyzed, with canyons interpolated by gravity and canyons north of 62° (Arctic canyons) omitted from the analyses (Fig. S1; S3; S4).

Sediment deposition within some of the canyons, forming internal terrace and levee deposits (e.g. Hansen et al., 2015), led to areas of steep positive slope within some mapped canyon profiles that do not represent the thalweg. Sampling below bathymetric resolution also created areas of flat slope that similarly do not represent the thalweg. A correction was applied to each profile to remove flat and upstream slopes and create a continuous downstream slope, thus better representing the canyon thalweg (Fig. 3). If the correction resulted in a concavity change of greater than 0.01 (~0.2 std. dev of all the errors) then the canyon was omitted from the analysis, under the assumption that the intra-canyon deposition was too severe to allow for a reliable concavity measurement (Fig. 3; Fig. S1; S2). These omissions, coupled with the soundings omissions, result in 555 canyons being selected from the original 5849 mapped by Harris and Whiteway (2011). The criteria used for these omissions is strict, but aims to greatly improve the reliability of the results. The corrected, uncorrected and omitted profiles and their concavities of all 5849 canyons have also been recorded (Fig. S3; supplementary data).

The concavity of each profile is represented by the normalized concavity index (NCI), which measures the elevation difference between a straight line fitted between the most upstream and downstream profile points, and the measured profile (Chen et al., 2019):

$$NCI = median[\frac{(E_L - Y_L)}{(E_0 - E_n)}] \quad \text{(Eq. 2)}$$

where E_L is the depth at each point on the measured profile, Y_L is the depth at each point on the fitted straight line, E_0 is the most upstream point of the measured profile, and E_n is the most downstream point of the measured profile. Linear profiles therefore have an NCI value of zero, while more concave profiles have more negative values, and more convex profiles have more positive values (Fig. 1B; 3; 4).

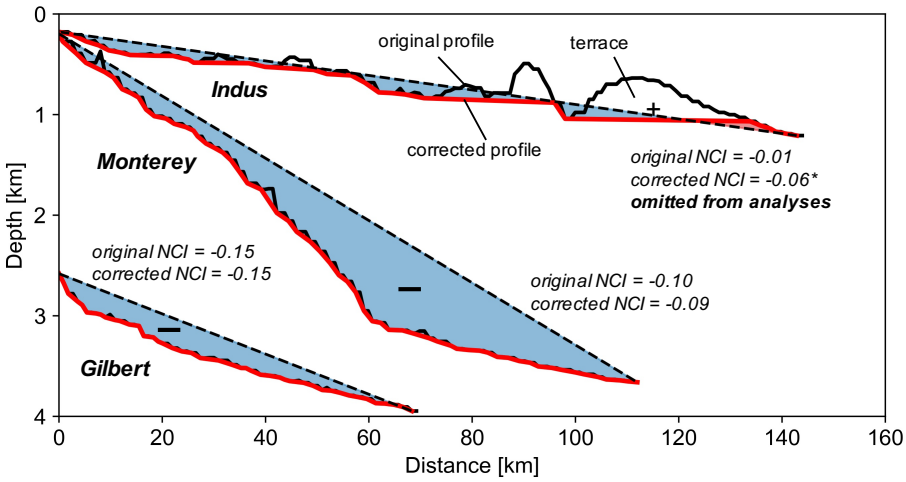

Figure 3: Three long profiles generated by this study and the correction applied to them to remove terrace deposition and irregular mapping. The original normalized concavity index (NCI) and the corrected NCI are shown.

2.3 Underlying controls

Following the methods used to assess the global controls on subaerial concavities (Chen et al., 2019; Seybold et al., 2020), each submarine canyon profile and its concavity was spatially merged with a number of different geomorphological, climatic and tectonic datasets (Fig. 2A). Canyon specific geomorphological variables, such as sinuosity and position on the slope, are from Harris and Whiteway (2011), while more general geomorphological variables, such as onshore relief, shelf gradient, and basin type are taken from Nyberg et al. (2018). Climatic impacts on concavity were assessed by joining each profile to its nearest onshore Koppen climate zone (Fig. 2A) (Kottek et al., 2006), mean annual precipitation value (Fick and Hijmans, 2017), and aridity index (Zomer et al., 2008).

The impact of tectonics on concavity was assessed through grouping of canyons by the basin-type in which they are located (Nyberg et al., 2018), and pairing them with onshore seismicity (peak-ground-acceleration with 10% chance of exceedance in 50 years; Giardini et al., 1999) (Fig. 2B). An additional basin-type was differentiated within the framework of Nyberg et al (2018) to represent canyons formed on the salt-deformed north slope of the Gulf of Mexico passive margin. While this nearest pairing method discounts factors such as the dominant climate regime of the drainage basin to individual canyons, it is the most consistent way to pair canyons located in variable offshore positions on a global scale. More targeted case studies would be needed to understand canyon morphology at a smaller scale (e.g. offshore California).

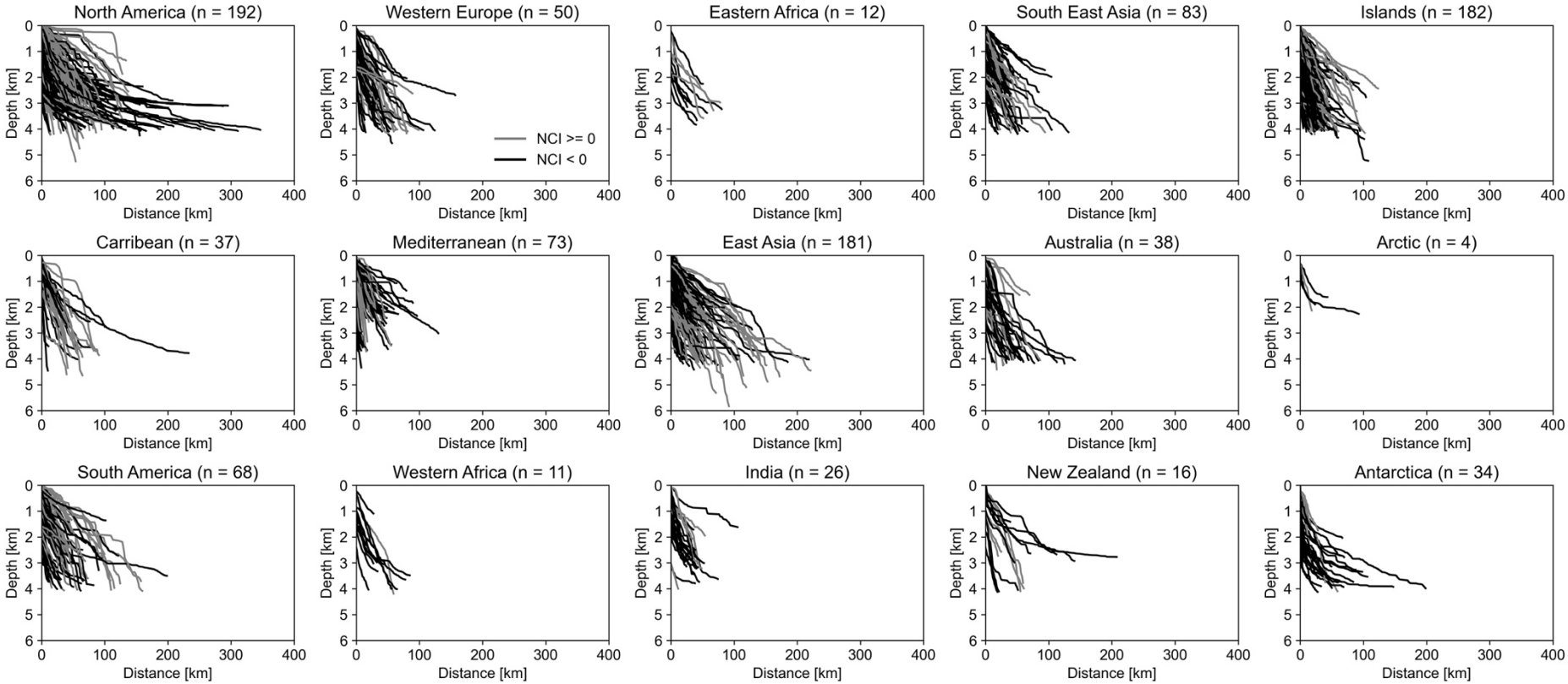

Figure 4: All long profiles generated by this study from each geographic location as defined by Harris and Whiteway (2011).

2.4 Statistics

Plots of the kernel density estimation (KDE) of grouped canyon concavities were used to visually compare their differences, with the median of each distribution plotted as a straight vertical line (Fig. 6). Two-sample Kolmogorov–Smirnov (KS) tests (e.g. Massey Jr, 1951) and the resulting probability values (p-values) were used to assess significance of differences between different distributions, with lower p-values indicating more significant differences. Spearman rank coefficients (ϱ) were used to assess positive or negative correlations between canyon concavity and geomorphic, tectonic and climatic variables (Fig. 9). The strength of the correlation was evaluated by the p-value derived from the correlation. In order to assess for correlations that may be obscured by local variation (Seybold et al., 2020), canyons were also binned and their indices averaged (median) by geographic location (e.g. Western North America) (Fig. 9) and by UTM zone.

3. Results

Detailed descriptions and interpretations of the mapped submarine canyons, such as their lengths, spacings and sinuosity, are documented in Harris and Whiteway (2011). The following sections will therefore focus on their longitudinal profiles.

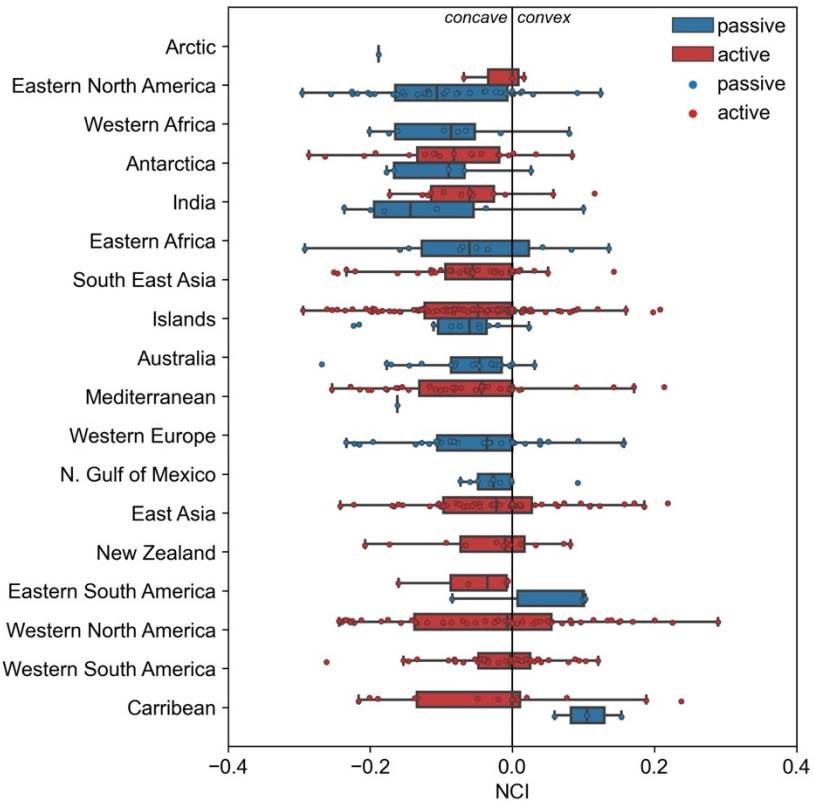

Figure 5: Box-plot showing the NCI quartiles, median and outliers for each geographic region.

3.1 Tectonics

Longitudinal profiles were collected, and normalized concavity indices (NCI) calculated, for 555 submarine canyons (Fig. 4). The median NCI of canyons is -0.04, indicating that most submarine canyons are concave. Submarine canyons formed on passive margins (median NCI = -0.07) are more concave than those formed on active margins (median NCI = -0.03, p = 0.02) (Fig. 6A). Canyons formed on the eastern North American passive margin are the most concave (if n > 10), and canyons formed on the western South American convergent margin and in the Caribbean are the least concave (Fig. 5). This is highlighted when canyons are grouped by basin type, with forearc basin canyons being statistically the least concave, and passive margin canyons the most concave (Fig 6B). Canyons formed on islands and in intracratonic, diapiric, foreland basins have differing

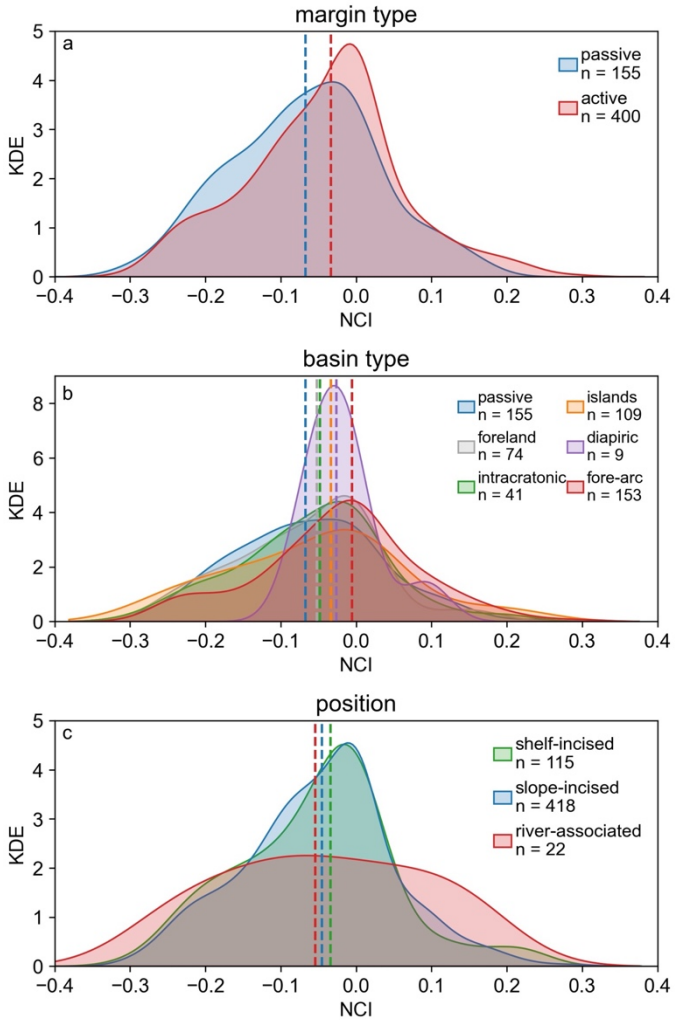

Figure 6: Kernel density estimations (KDE) of the NCI for grouped canyon concavities: a) active and passive margins, b) basin type, c) canyon position. Vertical line is the median.

concavity distributions, but their differentiation is less significant compared to all other canyons (Fig. 7A).

The influence of tectonics is also evident through the strong negative correlation between concavity and onshore seismicity, and the weak positive correlation between concavity and margin sediment thickness for each geographic region (Fig. 8). This is in contrast to the relationship observed within fluvial systems on a global-scale (Seybold et al., 2020), where concavity increases with increasing seismicity. It should be noted that these correlations are only present when canyons are binned by geographic location, and not when taken individually or binned by UTM-zone, indicating significant local variation or dilution of the correlation across drainage basins (Fig. S3).

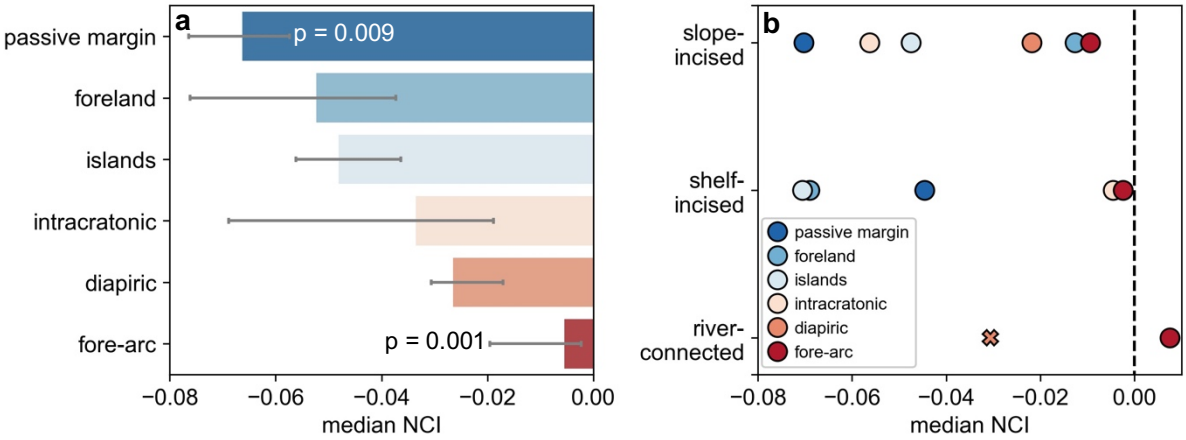

Figure 7: : A) Median NCI values for canyons formed in each basin type. Error bar indicates 68 % confidence interval. B) Median NCI values for each basin type grouped by their position on the slope. River-associated canyons formed on active margins more convex than shelf- and slope-incised canyons formed on active margins.

3.2 Canyon position

Canyon position also plays a role in adjusting concavity. Slope-incised and shelf-incised submarine canyons, which at present day are dissociated from rivers, have less variation in concavity (std. dev. = 0.10) than shelf-incised submarine canyons with a present-day connection to a river system (std. dev. = 0.13) (Harris and Whiteway, 2011). Shelf-incised and slope-incised canyons are more statistically similar (Fig. 6C). Where the number of river-associated, shelf-incised, and slope-incised canyons is greater than 10 for an individual basin-type (forearc basins), river-association appears to result in less concave canyons (Fig. 7B).

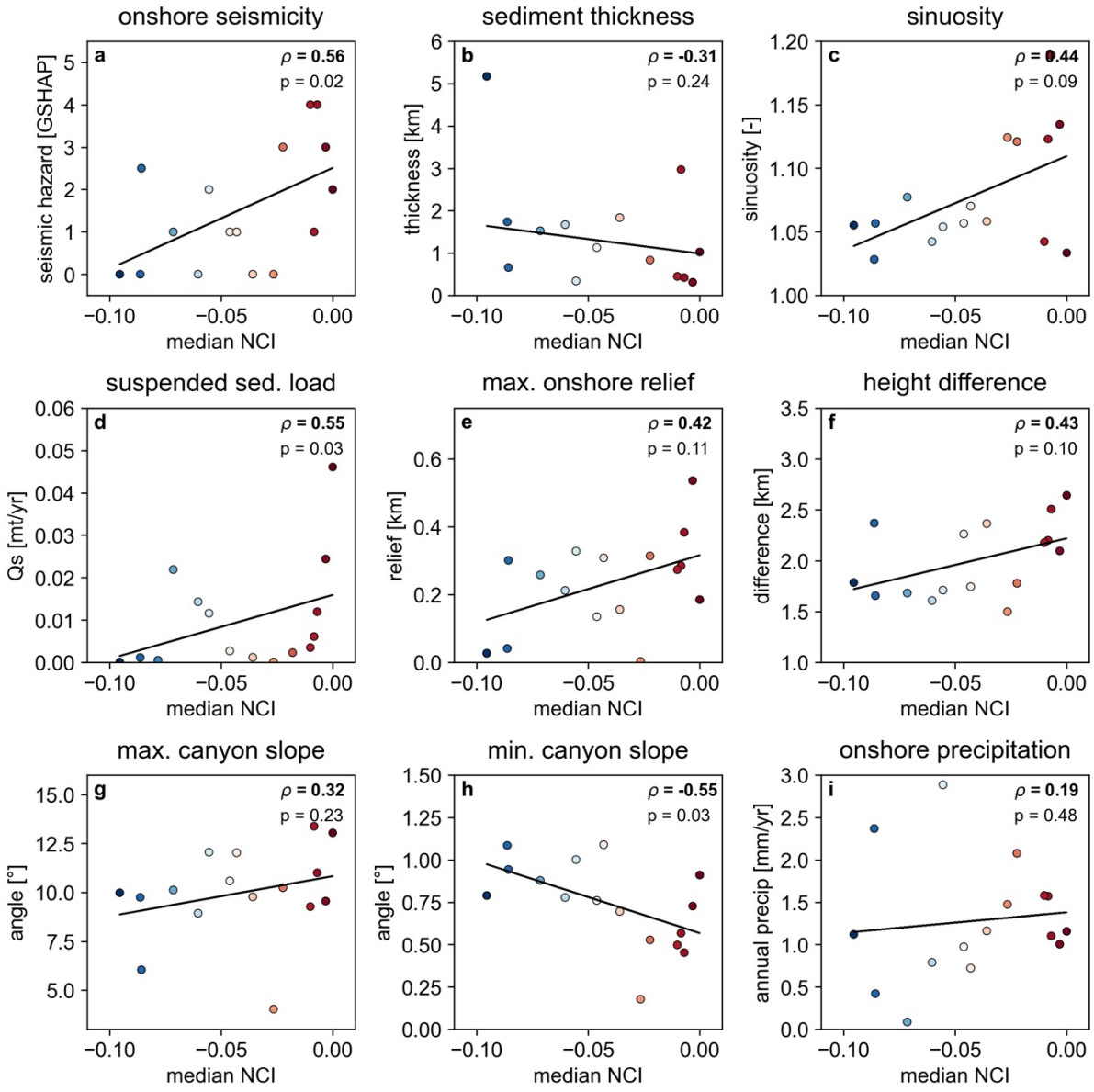

Figure 8: Correlation between canyon NCI and various climatic and tectonic indices (Giardini et al. 1999; Harris and Whiteway, 2011; Fick and Hijmans, 2017; Nyberg et al. 2018). Each canyon has been binned into their geographic region (e.g. Western South America (WSA) and Eastern North America Africa (ENA)) and median values taken. Spearman rank correlation (ϱ) is shown in bold, black solid line is a linear regression. Islands are omitted due to their geographical range.

3.3 Climate

When grouped by their nearest subaerial climate zone, canyons show a wide range of different deviations that are either not statistically significant, contradictory or not maintained across groups (Fig 10). The most prominent climatic deviation is seen on passive margins, with passive margin canyons formed adjacent to continental climates, such as NE America and Scandinavia, statistically more concave than canyons formed in other climates (Fig. 9). The opposite of this trend is seen in forearc basins, however, where continental canyons are statistically more convex. When river-

associated canyons are isolated, a relatively strong negative correlation is documented between concavity and onshore temperature (Fig. S4).

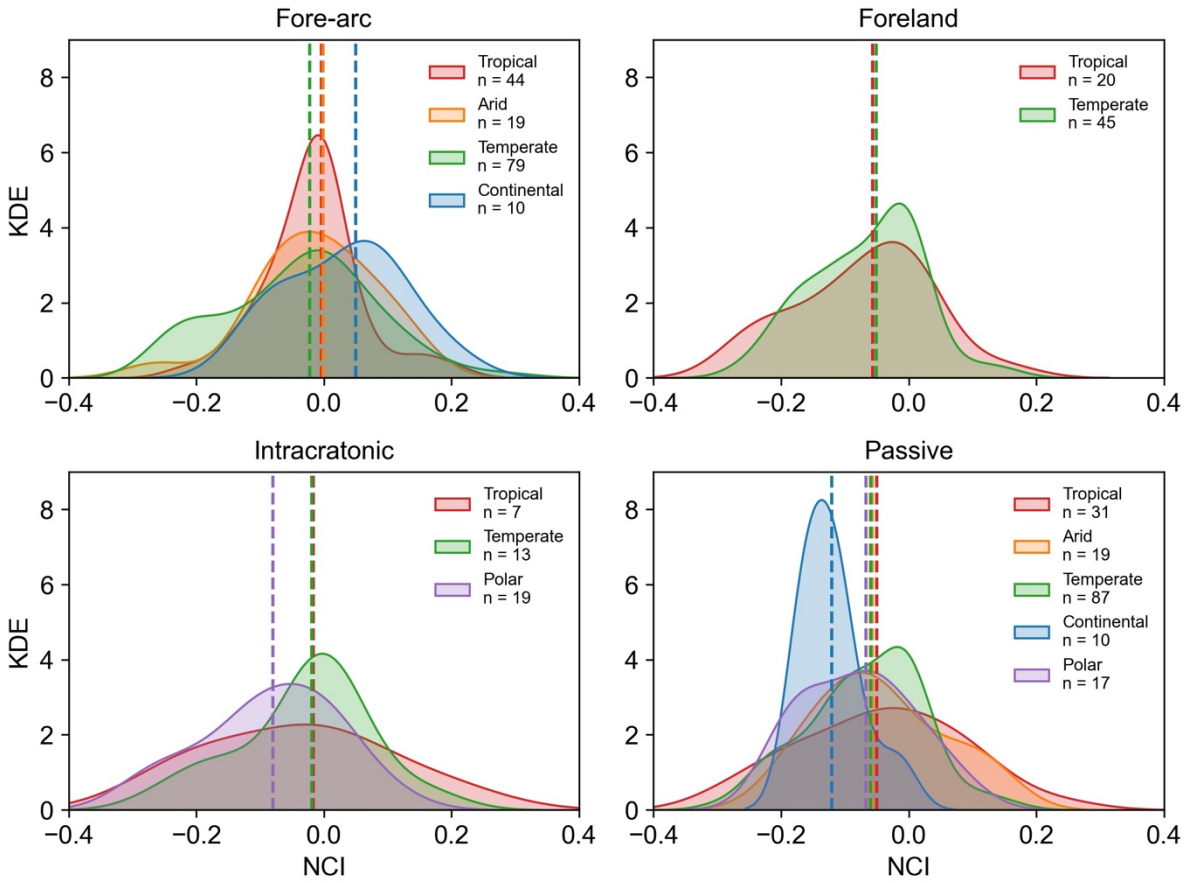

Figure 9: Kernel density estimations (KDE) of the NCI for each canyon grouped by basin type and climate zone. There is a wide variation in climate influence for each basin, indicating other factors, such as tectonics, are more important. Dashed line is the median.

3.4 Other factors

When concavity is compared against other indices, statistically significant correlations are rare, and only observed between concavity and minimum canyon slope on a margin-scale (Fig. 8). This relationship is not preserved on smaller-scales, such as across UTM zones (Fig. S4). No strong correlations are observed between other geomorphological variables, such as canyon dendricity, shelf width, shelf gradient, and slope gradient, suggesting that these properties do not have a strong influence on submarine concavity morphology on a global- or continental-scale (Fig. S4). When river-associated canyons are isolated, relatively strong positive correlations are documented between dendricity and concavity (Fig. S4).

4. Discussion

Two ratios help to elucidate the processes controlling the concavity of submarine canyons: 1) the ratio between seafloor deformation and downslope current capacity, and 2) the ratio between sedimentation and downslope current capacity. Canyons become more concave when downslope currents have greater capacity to erode and/or transport sediment downslope, and become less concave when currents have insufficient capacity to erode or transport sediment downslope.

4.1 Tectonism and erodibility

When the rate of seafloor deformation exceeds the capacity of currents in the canyon to erode the substrate, canyons are expected to be less concave. This is revealed by the decreased concavity of submarine canyons formed on convergent margins (Fig. 7A; 10), which are commonly undergoing active seafloor deformation through folding, faulting or accretionary prism formation (e.g. Pirmez et al., 2000; Covault et al., 2011). The Sinú accretionary prism, Colombia (Vinnels et al., 2010), and the Cook Strait, New Zealand (Micallef et al., 2014), are examples of such a process, with thrust faulting modifying the profiles of incisional submarine canyons and channels, causing them to be convex. The erodibility of these margins is also expected to play a role in adjusting canyon morphology, with the weak correlation between sediment thickness and concavity possibly a consequence of the thinner erodible sediment cover seen on active margins causing a decrease in canyon concavity (Fig. 8). The decreased concavity seen in the Caribbean canyons may also be partially attributed to substrate lithology, with the carbonate shelves that characterise much of the Caribbean expected to be less erodible than siliciclastic shelves.

On passive margins, where seafloor deformation is limited to relatively few gravitationally-deforming examples (e.g. Rowan et al., 2004), such as the Niger Delta (e.g. Adeogba et al., 2005; Mitchell et al., 2020), submarine canyons are generally more concave (Fig. 21), because the relatively minor or slowly-deforming seafloor topography is able to be eroded by downslope currents. On the diapiric Gulf of Mexico passive margin (e.g. Prather et al., 2017) concavities are similar to those seen on convergent margins. This indicates that the rate of seafloor deformation induced by salt diapirism outpaces the rate at which flows through these canyons can erode (Fig. 21).

A weak positive correlation also exists between NCI and onshore seismicity, i.e., canyons become less concave with increasing onshore seismicity (Fig. 8). The opposing trend is documented in subaerial river profiles, with increasing tectonic activity resulting in a global trend toward increasing concavity as headwaters are uplifted and steepened (Seybold et al., 2020). This discrepancy may be attributed to the greater degree of uplift in the uplands of tectonically-active subaerial

environments compared with adjacent submarine environments, which is demonstrated by calculating the elevation of a long profile as a function of uplift gradient (Eq. 1; Fig. 1A). When the uplift gradient is varied from upstream-focused (> 0) to downstream-focused (< 0) the profiles become increasingly more convex (Fig. 1A), with NCI values that are equivalent to the median of forearc canyons when the downstream uplift gradient is around 80% of its maximum in the example profile (Fig. 1B). This indicates that submarine canyons formed on convergent margins and adjacent to seismically-active margins are subject to uplift primarily in their downstream reaches, i.e., on the slope (Fig. 10). The increased concavity seen in canyons associated with islands may be explained by an upstream uplift gradient, with volcanic islands commonly characterised by Holocene uplift associated with isostatic rebound and magmatic underplating (e.g. Campos et al., 2010; Fretwell et al., 2010).

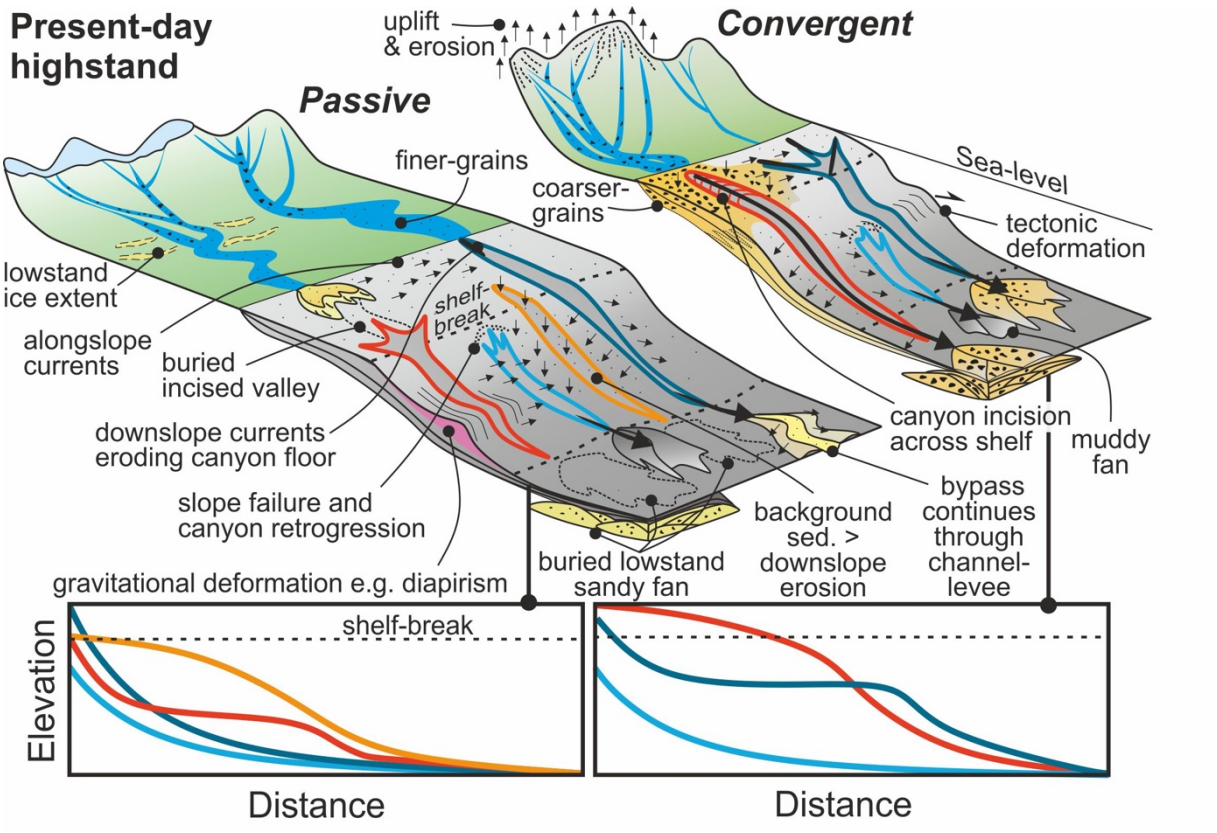

Figure 10: Schematic diagram showing the factors that may influence canyon concavity on convergent and passive margins during the present-day highstand. Passive margins have longer transfer zones, resulting in finer grains and enhanced bypass potential, while convergent margins have steeper and shorter transfer zones, resulting in coarser grains being stored in the canyon-head area and increased incision of canyons across the low-gradient shelf during highstand. Both convergent margins and passive margins may have tectonically deformed slopes, resulting in decreased concavity.

4.2 Sediment supply and character

When sediment supply exceeds the capacity of subaqueous currents to transport sediment downslope, or hemipelagic sedimentation exceeds the rate at which subaqueous currents can erode, canyons will become less concave as the upper slope aggrades (Gerber et al., 2009; Amblas et al., 2012) (Fig. 10). This may also contribute to the decreased concavity seen on convergent margins, with large volumes of sediment derived from uplifting hinterlands primarily deposited on the shelf and slope during the present-day highstand (Fig. 10). This is supported by a further decrease in concavity when forearc basins are associated with rivers (Fig. 7B), which deliver vast quantities of coarse sediment to oceans (e.g. Milliman and Syvitski, 1992). During highstand these coarse grains will be more difficult to transport down-canyon and along-slope from the river-mouth in littoral cells (e.g. Fisher et al. 2021), resulting in greater sedimentation rates on the shelf and upper slope, reduced sediment bypass to deeper water, and decreased canyon concavity (Fig. 10). This process is also suggested by the negative correlation between concavity and onshore seismicity, relief, and suspended sediment load (Fig. 8), as high supplies of coarse-grained sediment are expected from steep, tectonically-active hinterlands. These coarse-grained flows are also likely to be more erosive, however this erosion must be concentrated on the lower-gradient shelf during highstand, resulting in decreased concavity (Fig. 10). The weak negative correlation between concavity and sinuosity at the margin-scale may also reflect sediment supply, with canyons presently subject to high sediment supply and more frequent flows more likely to be sinuous than those presently stranded at the shelf-break far from sediment sources.

The impact of rivers on concavity may be reduced, or reversed, on passive margins due to the longer subaerial transport distances and finer grain-sizes delivered to most passive margins and their submarine fans (Reading and Richards, 1994) (Fig. 10). Finer grains are more easily transported along and downslope by submarine currents, which will result in more concave profiles than those formed where the sediment supply is similar but grain-sizes are larger. An example of this may be the river-associated Congo canyon on the west African passive margin, which is supplied with fine grained sediment from the Congo river (Azpiroz-Zabala et al., 2017), promoting bypass toward the Congo fan (Rabouille et al., 2019; Picot et al., 2019) and the development of a concave profile (Savoye et al., 2009). Discharge and sediment supply rates are also likely to be steadier on passive margins characterized by long transfer zones, as extreme climatic and tectonic events are more easily buffered (e.g. Romans et al., 2016). This will allow sediment to be more easily redeposited downslope before it is sequestered on the shelf or in the canyon, resulting in more concave profiles.

The influence of hemipelagic sedimentation in decreasing concavity may be apparent within some stranded passive margin canyons that are relatively linear or convex, such as those seen offshore western Australia and western Europe, with erosion by the now relatively infrequent downslope currents unable to keep pace with hemipelagic or along-slope sedimentation along these margins (e.g. Gerber et al. 2009).

4.3 Climate and sea-level

Onshore climatic effects appear to be masked by tectonics, position on the slope, or local factors in most cases (Fig. 9) indicating that onshore climate plays a subsidiary role in modifying the morphology of modern submarine canyons, or that canyons are responding to onshore climate change at a slower rate than tectonics or eustasy. In this way, submarine canyons are comparable to subaerial canyons, with tectonism obscuring any potential climatic impact of fluvial geomorphology on a global-scale (Seybold et al., 2020). Weak negative correlations between concavity and suspended sediment load, run-off, onshore relief and concavity are seen when the bin-size is widened to a continental-scale (e.g. Western North America), indicating some climatic influence through enhanced run-off and sediment supply at this scale. The correlation seen between greater onshore temperatures and decreased concavity within river-associated canyons support the relationship of climate and sedimentation, with greater chemical weathering causing enhanced sediment flux (Fig. S4). These relationships may not be causal, however, as higher sediment flux will be expected from active margins with greater and rejuvenated relief closer to the coast, and orographic precipitation. The influence of climate may therefore be difficult to disentangle from tectonics, as both are inextricably linked.

The most prominent climatic deviation is seen on passive margins, which are significantly more concave when adjacent to landmasses with continental climates, indicating substantial bypass through these canyons (Fig. 9). This can be attributed to the increased sensitivity of these climates to Quaternary glacial-interglacial transitions, which was noted by Covault et al. (2011) as an explanation for the concave high-latitude Astoria and Laurentian canyons. Much of the area subject to present-day continental climates (such as NE America) has lost up to 2.5 km of ice since 21 ka (Peltier, 2004; Gomez et al., 2020), which will have promoted high sediment supplies to these margins (Piper and Normark, 2009). Much of this sediment was bypassed through the canyons, forming their concave profiles and extensive submarine fans (Skene and Piper, 2003).

This conclusion results in a contrast, with passive margin canyons subject to high sediment supplies hosting more concave profiles, and forearc canyons subject to high sediment supplies hosting less concave profiles. This indicates that either: 1) grain-sizes are much lower on high-

supply passive margins and subaqueous currents are more able to transport the sediment downslope, or 2) these passive margin canyons were active when sediment bypass potential was greater. Since coarse sediments are known to have been supplied to these passive margin canyons during glacial periods (Piper and Normark, 2009), the latter explanation is more likely, and is suggested to be the result of sea-level variation.

Sediment bypass to deep-water is known to be tied to relative sea-level changes, with rivers able to traverse the shelf and deliver sediment more easily to the shelf-edge and deeper waters during lowstands. The present-day global highstand has resulted in enhanced accommodation on the shelf, therefore younger canyons, like those forming on active margins, are active when sedimentation on the shelf is enhanced and bypass to deeper water is hindered. Older canyons, however, were primarily active during the last lowstand when accommodation on the shelf was reduced and bypass to deeper-water was enhanced by sea-levels up to 120 m lower than present (Lambeck and Chappell, 2001; Miller et al., 2020). Lowstand canyons now pinned to the shelf-break will therefore be more concave than canyons active during the present-day highstand.

The incised valleys that fed these lowstand canyons are likely buried on the shelf, enhancing their concavities by preservation of only the steepest sections of the canyon on the slope (Fig. 10). On active margins, where incised valleys are expected to be deeper owing to steeper river gradients, canyons can be more easily traced onto the shelf as the incised valley is less likely to be fully buried during transgression and highstand (Fagherazzi et al., 2004; Harris and Whiteway, 2011) (Fig. 10). Canyons formed on active margins with narrow and steep shelves are also more prone to maintaining connection with the shoreline during Holocene transgression (Bernhardt and Schwanghart, 2021). Therefore, some of the decreased concavities seen in active margin canyons may be attributed to the combination of preferential preservation of incised valley relief on the shelf and an increased ability of these canyons to incise across the shelf (Fig. 10).

4.4 Slope-incised canyon processes

Many slope-incised canyons currently dissociated from rivers are unlikely to have been associated with rivers even during relative sea-level falls of Quaternary magnitudes (< 120 m lower), yet they are consistently concave (Fig. 6C), indicating erosion and bypass of subaqueous currents. Since slope-incised canyons are largely disconnected from rivers, the currents in these canyons must be formed by other processes, such as dense shelf-water cascades (e.g. Canals et al. 2006, Puig et al., 2008), nepheloid layers (Warratz et al., 2019), capture of along-slope currents (e.g. Marchès et al. 2007), or through retrogressive failure of the canyon walls (Sultan et al., 2007; Carter et al., 2018) (Fig. 10).

Mechanisms for producing concave profiles in slope-incised canyons were discussed by Adams and Schlager (2000), Mitchell (2004; 2005), and Brothers et al. (2013), who hypothesized that the downstream transition from weakly-erosive debris flows, derived from canyon head failures, to highly-erosive turbulent flows would result in increased erosion of the canyon profile downstream and more concave long profiles. This study supports these findings, indicating that many canyons evolve predominantly through processes unrelated to terrigenous sediment supply. It should also be noted that many lowstand canyons that were previously river-associated may now be evolving according to this process during highstand, thus increasing their concavity through time.

5. Conclusion

Modern submarine canyon longitudinal profiles and their concavities have been measured globally. The dominant control on global submarine canyon morphology is onshore tectonic activity and configuration, with forearc basins hosting the least concave canyons, and passive margins the most concave canyons. The reduced concavity seen in forearc basins is attributed to: 1) high supplies of coarse-grained sediment during the present-day highstand, resulting in both erosion and deposition being concentrated on flooded, low-gradient shelves, and 2) the rate of slope deformation being greater than the erosion rate of downslope currents. Concavity may also be decreased on passive margins by enhanced background sedimentation and gravitational deformation. Canyon position on the slope forms a secondary control on submarine canyon concavity, with shelf-incised canyons currently associated with rivers showing greater morphological variance than both shelf-incised canyons currently dissociated from rivers and slope-incised canyons, which have similar morphologies. This suggests that fluvial systems of different types are differentially influencing canyon morphology during highstand, and that many canyons are still 'frozen' in their lowstand morphology. These factors are difficult to disentangle from climate in most cases; however, climate has a pronounced influence on canyons formed adjacent to landmasses with major ice loss and high sediment flux during the Quaternary.

ACKNOWLEDGEMENTS

Datasets compiled for this study are available in the supplementary files (Tables S1 and S3) and in an online repository (Tables S1 to S3; https://doi.org/10.6084/m9.figshare.14338895). Source data is available from Harris and Whiteway (2011) (original submarine canyon data), Nyberg et al. (2018) (geomorphological, tectonic & climatic data), Kottek et al. (2006) (Koppen climate zones), Fick and Hijmans (2017) (precipitation data), Zomer et al. (2008), (aridity index), Giardini et al. (1999) (onshore seismicity), and Amanke and Eakins (2009) (bathymetry).

The authors thank the Slope project Phase 5 sponsors for financial support: Aker BP, BHP, BP, CNOOC, Hess, Murphy, Neptune Energy, Vår Energi, Wintershall DEA. Neil Mitchell is thanked for comments on an earlier version of the manuscript.

REFERENCES

Adams, E.W. and Schlager, W. (2000). Basic types of submarine slope curvature. *Journal of Sedimentary Research. 70*, 814-828.

Adeogba, A.A., McHargue, T.R. and Graham, S.A. (2005). Transient fan architecture and depositional controls from near-surface 3-D seismic data, Niger Delta continental slope, *AAPG Bulletin. 89*, 627-643.

Amante, C., Eakins, B.W. (2009). ETOPO1 1 Arc-Minute Global Relief Model: Procedures, Data Sources and Analysis. NOAA Technical Memorandum. National Oceanic and Atmospheric Administration, p. 19.

Amblas, D., Gerber, T.P., De Mol, B., Urgeles, R., García-Castellanos, D., Canals, M., Pratson, L.F., Robb, N. and Canning, J. (2012). Survival of a submarine canyon during long-term outbuilding of a continental margin. *Geology*, *40*, 543-546.

Azpiroz-Zabala, M., Cartigny, M.J., Talling, P.J., Parsons, D.R., Sumner, E.J., Clare, M.A., Simmons, S.M., Cooper, C. and Pope, E.L. (2017). Newly recognized turbidity current structure can explain prolonged flushing of submarine canyons. *Science advances, 3*, e1700200.

Bernhardt, A. and Schwanghart, W., (2021). Where and Why Do Submarine Canyons Remain Connected to the Shore During Sea-level Rise? Insights from Global Topographic Analysis and Bayesian Regression. *Earth and Space Science Open Archive.*

Brothers, D.S., Uri, S., Andrews, B.D., Chaytor, J.D. and Twichell, D.C. (2013). Geomorphic process fingerprints in submarine canyons. *Marine Geology, 337*, 53-66.

Campos, T.F., Bezerra, F.H., Srivastava, N.K., Vieira, M.M. and Vita-Finzi, C. (2010). Holocene tectonic uplift of the St Peter and St Paul Rocks (Equatorial Atlantic) consistent with emplacement by extrusion. *Marine Geology, 271,* 177-186.

Canals, M., Puig, P., de Madron, X.D., Heussner, S., Palanques, A. and Fabres, J. (2006). Flushing submarine canyons. *Nature*, 444, 354-357.

461 Carter, G.D., Huvenne, V.A., Gales, J.A., Iacono, C.L., Marsh, L., Ougier-Simonin, A., Robert, K.
462 and Wynn, R.B. (2018). Ongoing evolution of submarine canyon rockwalls; examples from the
463 Whittard Canyon, Celtic Margin (NE Atlantic). *Progress in Oceanography*, 169, 79-88.

464 Chen, S.A., Michaelides, K., Grieve, S.W. and Singer, M.B. (2019). Aridity is expressed in river
465 topography globally. *Nature, 573*, 573-577.

466 Covault, J.A., Fildani, A., Romans, B.W. and McHargue, T. (2011). The natural range of submarine
467 canyon-and-channel longitudinal profiles. *Geosphere, 7*, 313-332

468 Deng, A., & Stauffer, D. R. (2006). On improving 4-km mesoscale model simulations. *Journal of*
469 *Applied Meteorology and Climatology*, *45*(3), 361–381. https://doi.org/10.1175/JAM2341.1

470 Dietrich, W.E., Bellugi, D.G., Sklar, L.S., Stock, J.D., Heimsath, A.M. and Roering, J.J. (2003).
471 Geomorphic transport laws for predicting landscape form and dynamics: *Geophysical Monograph-*
472 *American Geophysical Union. 35*, 103-132.

473 Divins, D., 1998, Total Sediment Thickness of the World's Oceans and Marginal Seas. NOAA
474 National Geophysical Data Center.

475 Fagherazzi, S., Howard, A.D., Wiberg, P.L. (2004). Modeling fluvial erosion and deposition on
476 continental shelves during sea level cycles. *Journal of Geophysical Research, 109,* F03010.

477 Fick, S.E. and Hijmans, R.J. (2017). WorldClim 2: new 1-km spatial resolution climate surfaces for
478 global land areas. *International Journal of Climatology, 37*, 4302-4315.

479 Fisher, W.L., Galloway, W.E., Steel, R.J., Olariu, C., Kerans, C. and Mohrig, D. (2021). Deep-water
480 depositional systems supplied by shelf-incising submarine canyons: Recognition and significance
481 in the geologic record. *Earth-Science Reviews*, 103531.

482 Fretwell, P.T., Hodgson, D.A., Watcham, E.P., Bentley, M.J. and Roberts, S.J. (2010). Holocene
483 isostatic uplift of the South Shetland Islands, Antarctic Peninsula, modelled from raised beaches.
484 *Quaternary Science Reviews, 29*, 1880-1893.

485 Georgiopoulou, A. and Cartwright, J.A. (2013). A critical test of the concept of submarine
486 equilibrium profile. *Marine and Petroleum Geology, 41*, p. 35-47.

487 Gerber, T.P., Amblas, D., Wolinsky, M.A., Pratson, L.F. and Canals, M. (2009). A model for the
488 long-profile shape of submarine canyons. *Journal of Geophysical Research: Earth Surface*, 114(F3).

Giardini, D., Grünthal, G., Shedlock, K. M., & Zhang, P. (1999). The GSHAP global seismic hazard map. *Annals of Geophysics, 42*, 1225–1230.

Gomez, N., Weber, M.E., Clark, P.U., Mitrovica, J.X. and Han, H.K. (2020). Antarctic ice dynamics amplified by Northern Hemisphere sea-level forcing. *Nature, 587,* 600-604.

Hansen, L.A., Callow, R.H., Kane, I.A., Gamberi, F., Rovere, M., Cronin, B.T. and Kneller, B.C., (2015). Genesis and character of thin-bedded turbidites associated with submarine channels. *Marine and Petroleum Geology*, *67*, 852-879.

Harris, P.T. and Whiteway, T. (2011). Global distribution of large submarine canyons: Geomorphic differences between active and passive continental margins. *Marine Geology, 285*, p. 69-86.

Huyghe, P., Foata, M., Deville, E., Mascle, G. and Group, C.W. (2004). Channel profiles through the active thrust front of the southern Barbados prism. *Geology*, *32*, 429-432.

Kottek, M., Grieser, J., Beck, C., Rudolf, B. and Rubel, F. (2006). World map of the Köppen-Geiger climate classification updated. *Meteorologische Zeitschrift*, *15*, 259-263.

Lambeck, K. and Chappell, J. (2001). Sea level change through the last glacial cycle. *Science, 292*, 679-686.

Mackin, J.H. (1948). Concept of the graded river. *GSA Bulletin, 59*, p. 463–512.

Marchès, E., Mulder, T., Cremer, M., Bonnel, C., Hanquiez, V., Gonthier, E., & Lecroart, P. (2007). Contourite drift construction influenced by capture of Mediterranean Outflow Water deep-sea current by the Portimão submarine canyon (Gulf of Cadiz, South Portugal). *Marine Geology*, *242*, 247-260.

Massey Jr, F.J. (1951). The Kolmogorov-Smirnov test for goodness of fit. *Journal of the American statistical Association*, *46*, 68-78.

Micallef, A., Mountjoy, J.J., Barnes, P.M., Canals, M. and Lastras, G. (2014). Geomorphic response of submarine canyons to tectonic activity: Insights from the Cook Strait canyon system, New Zealand. *Geosphere*, 10, 905-929.

Miller, K. G., Browning, J. V., Schmelz, W. J., Kopp, R. E., Mountain, G. S., & Wright, J. D. (2020). Cenozoic sea-level and cryospheric evolution from deep-sea geochemical and continental margin records. *Science advances*, v. *6*, 1346.

Milliman, J.D. and Syvitski, J.P. (1992). Geomorphic/tectonic control of sediment discharge to the ocean: the importance of small mountainous rivers. *The Journal of Geology, 100*, 525-544.

Mitchell, N.C. (2004). Form of submarine erosion from confluences in Atlantic USA continental slope canyons. *American Journal of Science*, *304*, 590-611.

Mitchell, N.C. (2005). Interpreting long-profiles of canyons in the USA Atlantic continental slope. *Marine Geology, 214*, 75-99.

Mitchell, W.H., Whittaker, A.C., Mayall, M., Lonergan, L. and Pizzi, M. (2020). Quantifying the relationship between structural deformation and the morphology of submarine channels on the Niger Delta continental slope. *Basin Research.* In press. Available online.

Nyberg, B., Helland-Hansen, W., Gawthorpe, R.L., Sandbakken, P., Eide, C.H., Sømme, T., Hadler-Jacobsen, F. and Leiknes, S. (2018). Revisiting morphological relationships of modern source-to-sink segments as a first-order approach to scale ancient sedimentary systems. *Sedimentary Geology, 373*, 111-133.

Ouchi, S. (1985). Response of alluvial rivers to slow active tectonic movement. *GSA Bulletin*, *96*, 504-515.

Peakall, J. and Sumner, E.J. 2015). Submarine channel flow processes and deposits: A process-product perspective. *Geomorphology*, *244*, 95-120.

Peltier, W.R. (2004). Global glacial isostasy and the surface of the ice-age Earth: the ICE-5G (VM2) model and GRACE. *Annu. Rev. Earth Planet. Sci.*, *32*, 111-149.

Picot, M., Marsset, T., Droz, L., Dennielou, B., Baudin, F., Hermoso, M., De Rafélis, M., Sionneau, T., Cremer, M., Laurent, D. and Bez, M. (2019). Monsoon control on channel avulsions in the Late Quaternary Congo Fan. *Quaternary Science Reviews, 204*, 149-171.

Piper, D. J., & Normark, W. R. (2009). Processes that initiate turbidity currents and their influence on turbidites: a marine geology perspective. *Journal of Sedimentary Research*, *79*(6), 347-362.

Pirmez, C., Beaubouef, R.T., Friedmann, S.J., Mohrig, D.C. and Weimer, P. (2000). Equilibrium profile and baselevel in submarine channels: examples from Late Pleistocene systems and implications for the architecture of deepwater reservoirs. *Global deep-water reservoirs: Gulf Coast Section SEPM Foundation 20th Annual Bob F. Perkins Research Conference*, 782-805.

546 Prather, B.E., O'Byrne, C., Pirmez, C. and Sylvester, Z. (2017). Sediment partitioning, continental
547 slopes and base-of-slope systems. *Basin Research, 29*, 394-416.

548 Puig, P., Palanques, A., Orange, D.L., Lastras, G. and Canals, M. (2008). Dense shelf water
549 cascades and sedimentary furrow formation in the Cap de Creus Canyon, northwestern
550 Mediterranean Sea. *Continental Shelf Research, 28,* 2017-2030.

551 Rabouille, C., Dennielou, B., Baudin, F., Raimonet, M., Droz, L., Khripounoff, A., Martinez, P.,
552 Mejanelle, L., Michalopoulos, P., Pastor, L. and Pruski, A. (2019). Carbon and silica megasink in
553 deep-sea sediments of the Congo terminal lobes. *Quaternary Science Reviews, 222*, 105854.

554 Ramsey, L.A., Hovius, N., Lague, D. and Liu, C.S. (2006). Topographic characteristics of the
555 submarine Taiwan orogen. *Journal of Geophysical Research: Earth Surface*, *111*(F2).

556 Reading, H.G. and Richards, M. (1994). Turbidite systems in deep-water basin margins classified
557 by grain size and feeder system. *AAPG bulletin, 78*, 792-822.

558 Roberts, G.G. and White, N. (2010). Estimating uplift rate histories from river profiles using
559 African examples. *Journal of Geophysical Research: Solid Earth,* 115(B2).
560
561 Roe, G.H., Montgomery, D.R. and Hallet, B. (2002). Effects of orographic precipitation variations
562 on the concavity of steady-state river profiles. *Geology, v. 30,* 143-146.
563
564 Romans, B.W., Castelltort, S., Covault, J.A., Fildani, A. and Walsh, J.P. (2016). Environmental
565 signal propagation in sedimentary systems across timescales. *Earth-Science Reviews*, *153*, 7-29.
566
567 Rowan, M.G., Peel, F.J., and Vendeville, B.C. (2004). Gravity- driven fold belts on passive margin.
568 *AAPG Memoir, 82,* 157–182.
569
570 Savoye, B., Babonneau, N., Dennielou, B. and Bez, M. (2009). Geological overview of the Angola–
571 Congo margin, the Congo deep-sea fan and its submarine valleys. *Deep Sea Research Part II: Topical*
572 *Studies in Oceanography, 56*, 2169-2182.
573
574 Seybold, H., Berghuijs, W.R., Prancevic, J.F., Kirchner, J.W. (2020). Global dominance of tectonics
575 over climate in shaping river longitudinal profiles. *EarthArXiv,*
576 https://doi.org/10.31223/osf.io/bj8kh.
577

578 Shaffer, J.P. (1995). Multiple hypothesis testing. *Annual review of psychology*, *46*, 561-584.\
579
580 Sinha, S.K. and Parker, G. (1996). Causes of concavity in longitudinal profiles of rivers. *Water*
581 *Resources Research*, *32*, 1417-1428.

582 Skene, K.I. and Piper, D.J. (2003). Late Quaternary stratigraphy of Laurentian Fan: a record of
583 events off the eastern Canadian continental margin during the last deglacial period. *Quaternary*
584 *International, 99,* 135-152.

585 Sklar, L., & Dietrich, W. E. (1998). River longitudinal profiles and bedrock incision models: Stream
586 power and the influence of sediment supply. *Geophysical Monograph-American Geophysical Union*, *107*,
587 237-260.

588 Snow, R.S., and Slingerland, R.L. (1987). Mathematical modeling of graded river profiles. *The*
589 *Journal of Geology*, *95*, 15-33.

590 Snyder, N.P., Whipple, K.X., Tucker, G.E. and Merritts, D.J. (2000). Landscape response to
591 tectonic forcing: Digital elevation model analysis of stream profiles in the Mendocino triple
592 junction region, northern California. *GSA Bulletin, 112,* 1250-1263.

593 Sultan, N., Gaudin, M., Berne, S., Canals, M., Urgeles, R. and Lafuerza, S. (2007). Analysis of slope
594 failures in submarine canyon heads: an example from the Gulf of Lions. *Journal of Geophysical*
595 *Research: Earth Surface,* 112(F1).

596 Warratz, G., Schwenk, T., Voigt, I., Bozzano, G., Henrich, R., Violante, R. and Lantzsch, H.
597 (2019). Interaction of a deep-sea current with a blind submarine canyon (Mar del Plata Canyon,
598 Argentina). *Marine Geology, 417*, 106002.

599 Whipple, K. X., & Tucker, G. E. (1999). Dynamics of the stream-power river incision model:
600 Implications for height limits of mountain ranges, landscape response timescales, and research
601 needs. *Journal of Geophysical Research: Solid Earth*, *104*(B8), 17661-17674.

602 Whittaker, A.C., Attal, M., Cowie, P.A., Tucker, G.E. and Roberts, G. (2008). Decoding temporal
603 and spatial patterns of fault uplift using transient river long profiles. *Geomorphology, 100,* 506-526.

604 Vincenty, T. (1975). Direct and inverse solutions of geodesics on the ellipsoid with application of
605 nested equations. *Survey review*, *23*(176), 88-93.

606 Vinnels, J.S., Butler, R.W., McCaffrey, W.D. and Paton, D.A. (2010). Depositional processes across
607 the Sinú accretionary prism, offshore Colombia. *Marine and Petroleum Geology, 27,* 794-809.

608 Yatsu, E. (1955). On the longitudinal profile of the graded river. *Eos, Transactions American*
609 *Geophysical Union, 36,* 655-663.

610 Zaprowski, B.J., Pazzaglia, F.J. and Evenson, E.B. (2005). Climatic influences on profile concavity
611 and river incision. *Journal of Geophysical Research: Earth Surface, 110(F3).*

612 Zomer, R.J., Trabucco, A., Bossio, D.A. and Verchot, L.V. (2008). Climate change mitigation: A
613 spatial analysis of global land suitability for clean development mechanism afforestation and
614 reforestation. *Agriculture, ecosystems & environment, 126,* 67-80.